An innovative method for soot deposit quantification using a CO2 sensor: application to fire studies in research facilities

Amel Kort, F-X. Ouf, Riadh Lakhmi, T. Gelain, J. Malet, Philippe Breuil, Jean-Paul Viricelle

An innovative method for soot deposit quantification using a CO_2 sensor: application to fire studies in research facilities

A. Kort[1, 2], F-X. Ouf[1, 3], R. Lakhmi[2], T. Gelain[1], J. Malet[1], P. Breuil[2], J-P. Viricelle[2]

[1]Institut de Radioprotection et de Sûreté Nucléaire (IRSN), PSN-RES, SCA, Gif-sur-Yvette, 91192, France
[2]Mines Saint-Etienne, Univ Lyon, CNRS, UMR 5307 LGF, centre SPIN, F-42023 Saint-Etienne, France
[3]Current affiliation : Laboratoire National de métrologie et d'Essais, Direction de la Métrologie Scientifique et Industrielle, 78190 Trappes, France

ABSTRACT

In industrial facilities handling or manufacturing hazardous materials, fires are one of the major hazards. Therefore, it is important to have tools to better understand the transport and deposition phenomenon of emitted particles in order to take into account their consequences on safety devices. For this purpose and due to the lack of quantitative soot deposition data under realistic fire conditions, an innovative method for soot quantification in experimental facilities devoted to fire research has been developed. This method is based on the quantification of gases emitted during regeneration of a resistive sensor surface and has a higher detection limit than the electrical conductance quantification method previously proposed and validated by (Kort et al., 2021). A proof of feasibility has been shown for two types of soot and a prediction curve has been proposed for deposited masses which vary between 16 and 350 µg (1304 mg.m^{-2} and 28525 mg.m^{-2}). The applicability of this measurement method to realistic industrial fire situation is finally verified taking into account the mean deposition mass per surface area observed in this context.

KEYWORDS

Gas sensor, soot, quantification, fire

1. INTRODUCTION

In industrial facilities handling or manufacturing hazardous materials (biological, chemical, nuclear, nanoscale…), fires are one of the major hazards when considering particles emission and dispersion in an airborne phase. Therefore, it is important to develop experimental and modeling tools to better understand the transport and deposition phenomenon of emitted particles in order to predict the consequences of such accidental situations and to implement relevant containment devices (high efficiency particulate air filters HEPA, physical barriers such as fire dampers or butterfly valves…) and strategies (pressure cascade, in depth defense…). For this purpose, development of simulation tools are currently in progress (Mensch & Cleary, 2019; Plagge et al., 2017) associated with specific prediction models of aerosol release/emission (Zepper et al., 2017), their transport (Gelain et al., 2021) and their deposition within industrial facilities or ventilation network (Overholt et al., 2016).

Beyond the question of aerosol fate during conventional industrial fires, special care is an absolute requirement for fires involving radioactive materials due to potential release of these materials in airborne phase. In such situations, assessment of radiation exposure/contamination of workers and release of radioactive materials in the environment must be carried out by predicting fire emitted particles inhalation in the human respiratory pathway and developing clogging models of HEPA filters since it is generally assumed as the last barrier of containment within a nuclear basic installation (NBI) before potential release in the atmosphere.

To support such developments, experimental data on soot deposition quantities and main mechanisms are crucial. Nevertheless, the lack of development and validation of measurement devices could be noticed, limiting the availability of relevant and quantitative information regarding mass per surface area of soot deposit formed under realistic fire conditions. Beyond limited technology readiness level of measurement devices, available soot deposition data are also limited to analytical combustion experiments (Riahi, 2012), medium scale fires performed in a marine container (Decoster, 2017) or in an office (Decoster et al., 2017). Mensch & Cleary (2018) used resistive sensors for a first attempt to quantify soot deposits formed by thermophoresis within a temperature

gradient imposed between thermally regulated rectangular flow chanel. According to this literature review, corresponding soot deposited mass per surface area are ranging from 20 to nearly 350 $mg.m^{-2}$, values confirming the relevance of the quantification method introduced by Kort et al. (2021). Nevertheless, additional measurements, carried out during real-scale and confined fire experiments (Kort et al., 2019) have demonstrated that significantly higher mass deposit (up to 25 $g.m^{-2}$) could be obtained under realistic conditions, limiting the range of application of the quantification method introduced by Kort et al. (2021).

Thus, the aim of this work is to develop an additional measurement devices able to quantify such high soot deposit contamination levels in a direct, non-invasive, representative and complementary way to the quantification method proposed by Kort et al., (2021).

This first experimental approach for an in situ quantification of soot deposition on walls during fires (Kort et al. 2021) is based on a resistive sensor previously developed in our consortium (Grondin et al., 2015).

The principle of this sensor is based on the conductance increase induced by the soot deposit formed between interdigitated electrodes when a polarization voltage is applied (Grondin et al., 2016).

In their study, Kort et al. (2021) adapted this technology for quantification of the soot particles' deposit and demonstrated its non-invasive behavior, regarding soot deposition mechanism for a defined range of polarization voltages. They also qualified a methodology to correlate the soot mass deposited onto the sensitive surface and the corresponding sensor's conductance value, opening the way to nearly real-time quantification of deposited mass of soot per surface area. For convenience, this method will be called "Electrical conductance" and will be particularly useful for predicting effects of soot deposit on safety elements such as electrical devices (Peacock et al., 2012).

The sensitive surface of the resistive sensor must be therefore frequently regenerated by burning the soot deposit at 650°C thanks to the heating resistance screen-printed on its back side to avoid conductance saturation reported by (Grondin et al., 2016). Similar asymptotic behaviour was also reported during tests carried out after the publication of (Kort et al., 2021) considering realistic soot emitted by burning organic solvents used for nuclear waste reprocessing (Tributylphosphate (TBP) / Hydrogenated Tetrapropylene (HTP) mixture) but for significantly lower deposited mass of soot on the resistive sensor sensitive surface.

To overcome these limitations and enhance the mass detection range to higher mass per surface area, an innovative quantification method is proposed in this study using gases emitted during the burn-off of soot deposit during the regeneration of the resistive sensor sensitive surface. The advantages of measuring the CO_2 during resistive sensor regeneration over using a gravimetric sensor after an exposure is that it provides information during the exposure (electrical measurement of resistive sensor) and then a quantification into the hermetically isolated cell by using a suitable sampling system. Moreover, with such a system, rapid cycles of sensor exposure/generation with CO_2 measurements could be applied, allowing a quasi-real time analysis with time frequency of a few minutes depending of the miniaturization level of the final sampling system.

The principle of the protocol proposed in this study is to correlate emitted gases concentration during soot oxidation with the corresponding mass of soot particles deposited on the sensing surface.

Thus, the chemical reactivity of soot and specifically its potential to be oxidized at a specific temperature will be discussed in the present study since it intervenes during the regeneration process. Several authors have studied and proposed suitable range of temperatures associated to the maximum loss of soot mass during their oxidation. According to (Müller et al., 2005), a reasonable assumption of temperatures range between 600 °C and 700 °C could be considered for a large variety of soot particles. In agreement with Müller et al. (2005), we will then consider a regeneration temperature of our resistive sensor of 650 °C.

Beyond the question of identifying the most relevant temperature for soot burn-off, oxidation of soot is a complex process due to their heterogeneous and versatile structure. Indeed, the chemical composition of soot emitted during fires can vary from organic to elemental carbon and the soot particle themselves can adsorb at their surface different kinds of complex organic molecules and even water ones (Lintis et al., 2021). Despite their complex nature, soot particles oxidation is generally assumed to produce mostly CO_2, CO and H_2O.

Since the method proposed in the present study is based on gases analysis during soot oxidation, thermogravimetric analyses coupled with mass spectroscopy analyses were performed on the two types of soot considered in the study: soot produced by a Mini-cast burner and soot produced by the combustion of TBP/HTP. These thermogravimetric analyses were carried out in order to determine the nature of the gases emitted during regeneration and to choose the most suitable technologies of gas sensors needed for this quantification method. Then, a specific transparent glass cell, coupling the resistive sensor with a regeneration tool and gas sensors to analyze the quantities of gas produced during the regeneration, was developed, qualified and validated for mass quantification purpose. A comparison between the present new method called "CO_2 emission" and the previous "Electrical conductance" method is finally proposed and discussed according to the level of mass deposition generally encountered during industrial fires, studied in research experimental facilities.

2. MATERIALS AND METHOD

2.1. Soot particles generation

The generated soot particles that will be quantified are representative, in terms of structure, size distribution and organic content (OC), of those produced during a fire involving fuels commonly encountered in the nuclear industry (Ouf et al., 2015).

The first type of soot particles was generated using a Mini-CAST burner (Jing 5201). In this case, the production of soot is based on a propane-air diffusion flame quenched by a nitrogen flow. The air, nitrogen and propane flowrates values define an operating point that can be modified to produce aerosols with different soot size distributions and chemical natures (Moore et al., 2014; Yon et al., 2015). The chosen operating point allowed generating soot with a small organic part, this latter being less conductive (Grondin et al., 2019). In the present study, the selected point is Q_{C3H8} =3.6 L.h^{-1}, $Q_{oxidation\ air}$ =90 L.h^{-1}, and $Q_{dilution\ air}$ =1200 L.h^{-1}. The median mobility diameter has been measured using a SMPS (Scanning Mobility Particle Sizer Spectrometer 3082 TSI). The median electrical mobility diameter of the particles is equal to 197 ± 6 nm with an average for the standard geometric deviation 1.6 ± 0.1, for the chosen working conditions of the Mini-Cast burner.
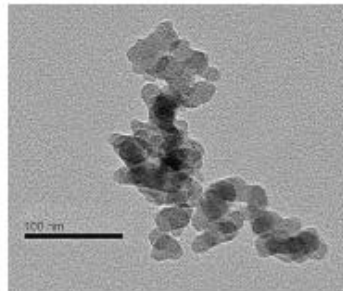

Figure 1 : TEM image of a CAST aggregate (from Brugière et al., 2014)

A second type of tested soot particles was produced by the combustion of the TBP (30%) /HTP (70 %) mixture. The test bench used for this production is described by (Lintis et al., 2021). The flow of oxidizing gas routed into the combustion chamber (0.03 m^3 in volume) is equal to 180 NL.min^{-1}. The residence time is about 10 seconds, which corresponds to a renewal rate of 400 h^{-1}. We begin the test by introducing the sample into the combustion chamber. The sample is therefore placed on the sample holder specified on a tared weighing cell. Data recording is synchronized with ignition. We recorded the size distribution using an SMPS (3082 TSI).

We reported a median electrical mobility diameter of 216 ± 15 nm and a standard geometric deviation of 1.5 ± 0.1. These particles present a size distribution similar to the one reported for the Mini-CAST soot but with a more complex chemical composition (Ouf et al., 2015) as illustrated in transmission electronic microscopy images reported in figures 1 and 2 with a clear evidence of nanodroplets located around TBP/HTP soot particles.
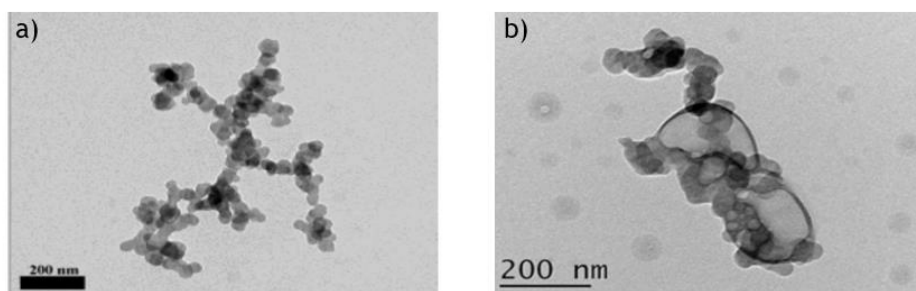

Figure 2 : TEM image of a TBP/HTP aggregate a) without adsorbed phase b) with adsorbed phase (from Ouf et al., 2015)

2.2. Choice of gas sensors

As previously mentioned, the proposed quantification method is based on the measurement of gases concentration emitted by the combustion of soot deposited on the sensor surface during the regeneration phase using the heating resistance of the sensor. Prior to such analyses, identification of gases to be quantified is needed to identify the most suitable gas sensors to be implemented.

For this purpose, and in order to characterize the thermal behavior of the soot produced by the Mini-CAST and of the combustion of TBP/HTP, thermogravimetric analyses (TGA) coupled with mass spectroscopy analyses (MS) were performed.

This type of analysis allows first to confirm the temperature of maximum oxidation proposed according to our literature analysis (650°C) and second, to identify the gaseous compounds emitted during the degradation of the studied soot particles. The used device is a TGA/DSC 1 thermobalance from Mettler coupled to a Omnistar GSD301 mass spectrometer.

The soot samples produced by the Mini-CAST and the combustion of TBP/HTP are steamed at 150 ° C for 1 hour. 6 mg of this sample are heated in synthetic air (air flow rate equal to 5 L. h^{-1}) up to 1200°C with a ramp of 10°C.min^{-1}. In order to assess repeatability, 3 identical tests were achieved. Figure 3 shows the thermogram obtained under air (left) and the mass spectrum (right) as a function of temperature for soot produced by the Mini-CAST. A single loss of mass occurs between 500 and 700°C, with a maximum rate of oxidation (97% of cumulative mass loss of the sample) associated with a temperature of about 620 ° C. This temperature appears in accordance with the one considered for the sensor's regeneration phase (650°C), making it possible to ensure the efficiency of this process. The main species produced in this temperature range is CO_2 (m / z = 44), resulting from the oxidation of carbon species composing the soot.
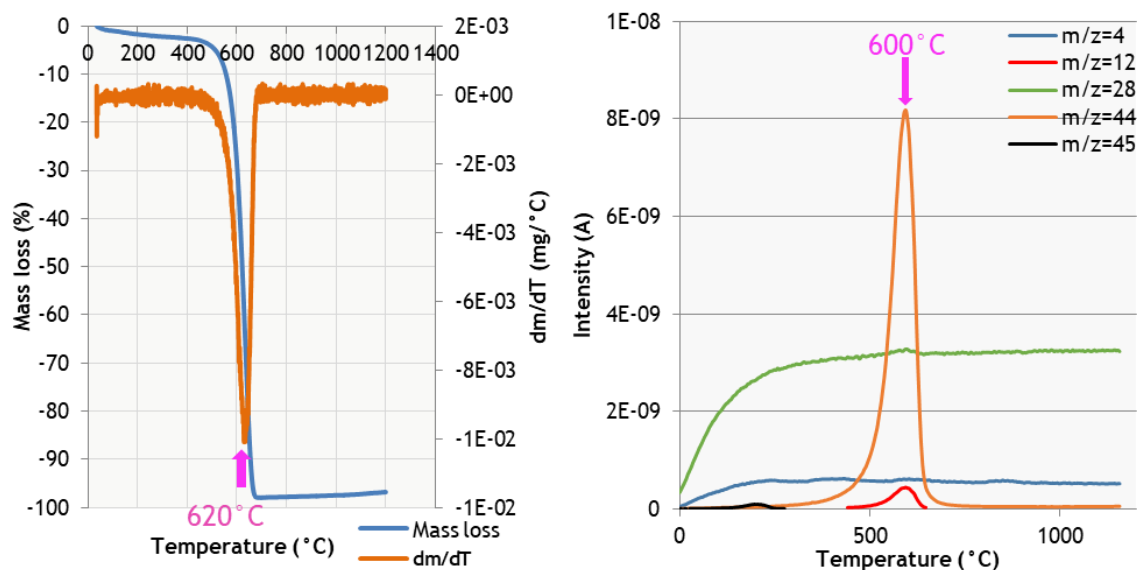

Figure 3 : Evolution of mass loss (TGA) (left) and mass Spectrum (right) under air as a function of temperature for soot produced by the Mini-CAST

The thermal behavior of TBP/HTP soot particles is shown in the thermogram obtained in figure 4, the analyses being carried out under the same conditions as the Mini-CAST soot. The thermal behavior of the TBP/HTP soot particles appears more complex than the one reported for soot produced by the Mini-CAST. This type of soot has a higher reactivity in a temperature range between 120 and 800 ° C. The existence of 4 temperature zones of mass losses is noted in TGA of figure 4. The first mass loss occurs between 30 and 90 °C, with a maximum rate of mass loss at around 57 °C.
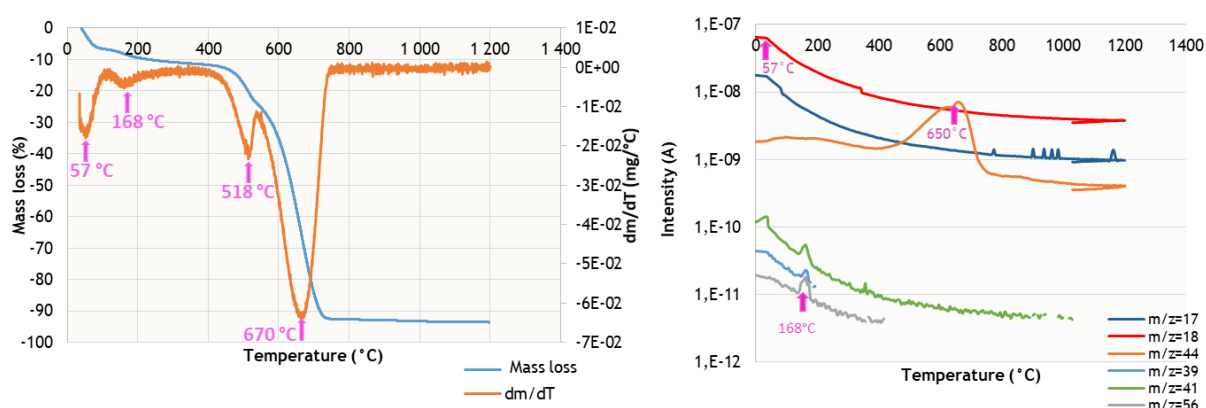
Figure 4 : Evolution of mass loss (TGA) (left) and mass Spectrum (right) under air as a function of temperature for soot produced by the combustion of TBP/HTP at 21% oxygen

The cumulative mass loss of 2 % can be attributed to the desorption of physisorbed water (m / z = 18) since TBP/HTP soot particles present significant amount of phosphor (Ouf et al., 2015) known to be active site for water molecules. Water has been re-absorbed after soot pretreatment. The second mass loss occurs between 120 and

4

230°C (maximum at 168°C) corresponding to a cumulative mass loss of 5% and which can be attributed to the production of "VOC" type species (volatile organic compounds, m / z = 39, 41, 56) difficult to identify from present MS analysis. The third mass loss cannot be dissociated from the fourth and the main one that occurs between 500 and 800°C with a maximum mass loss at 670°C (in accordance with the regeneration temperature of 650°C of the sensor) and corresponds to a cumulative loss of mass total of 93%. In agreement with Mini-CAST soot particles, the species produced in this temperature range is mainly CO_2 (m / z = 44) that could be associated with the degradation of carbon contained in soot for quantification purpose.

From the thermogravimetric analyses and mass spectroscopy analyses, we can conclude that the temperature of maximum mass loss due to the oxidation of studied soot can be assumed to be close to 650°C. Furthermore, at this temperature, soot oxidation mainly produces CO_2.

Following thermogravimetric analyses coupled with mass spectroscopy analyses, the main gas emitted during the combustion of CAST and TBP/HTP soot is CO_2. Consequently, a CO_2 sensor can be used as described by the protocol in part 2.3 to propose a correlation between the mass of soot present on the soot sensor sensitive surface and the mass of carbon calculated from the difference in CO_2 concentration before and after regeneration of the soot sensor. Therefore, we have selected a Sensirion SCD30 CO_2 sensor which also includes a temperature sensor and a humidity sensor. This CO_2 sensor is an optical one (NDIR for "Non-Dispersive Infrared Sensor") which uses an infrared source whose radiation passes through a gas-filled chamber, and the infrared detector retrieves the wavelengths corresponding to a CO_2 absorption band at the output thanks to an interference filter.

2.3. Principles and assumptions associated with the method

After identifying and choosing the most relevant gas sensor to correlate soot deposited mass with gas concentration encountered in a closed system during soot oxidation, a quantification protocol and a measurement cell were introduced. In order to draw a calibration curve for the proposed method, the following quantification protocol was used according to the four stages described in figure 5:
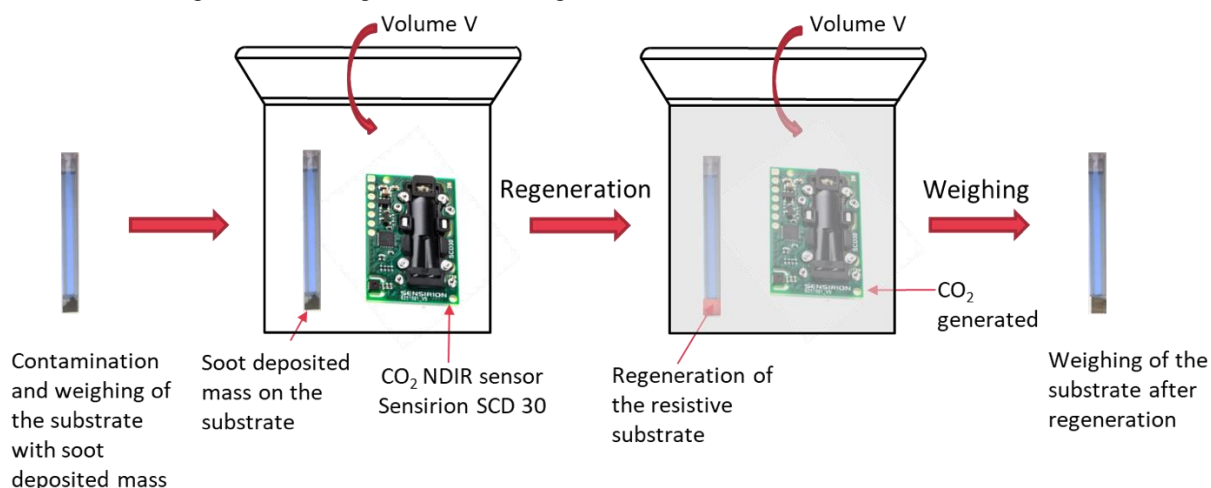

Figure 5 : Experimental protocol of CO₂ quantification

1 °) the contamination of sensor by Mini-CAST or TBP/HTP soot particles is based on a manual deposit protocol applied to the sensitive surface of the resistive sensor. The manual protocol consists in weighing a soot free sensor. Then, the non-sensitive surface of the sensor is protected by a parafilm to avoid any deposition of soot on the non-sensitive surface of the soot sensor. A mass of soot is set in a petri dish and the resistive surface of the sensor is manually contaminated. The parafilm is then removed and the non-sensitive surface of the sensor was additionally cleaned using a Chemtronics© micropoint cotton tip swab with a constant volume of 0.1 mL of ethanol (ethanol absolute anhydrous 99.9% from Carlo ERBA) to be totally sure that it is free of any soot deposit. Manually contaminated sensor was then weighed (Sartorius MC210P) to determine the mass of the system prior to regeneration in the measuring cell.

2 °) the contaminated sensor is introduced into the measuring cell for quantifying the mass of deposited soot. The deposited soot is brought to a temperature of 650°C thanks to the heater on the back face of the substrate and are thus oxidized. Since the cell is hermetically isolated, the CO_2 gas concentration in the cell reaches a steady state which is a function of the quantity of oxidized soot and cell volume. This concentration is continuously measured by the CO_2 sensor.

As demonstrated in our previous studies (Kort et al., 2021; Ouf et al., 2015), soot produced by the Mini-CAST or by the combustion of TBP/HTP consist mainly of carbon in an elemental form.

We also know, based on coupled TGA / MS analyses (figures 3 and 4), that the gas produced during regeneration is overwhelmingly CO_2.

Knowing the volume of the sensor cell (V = 0.4 ± 0.004 L), we calculate the number of moles of CO_2 (mol) Δn_{CO_2} generated by the combustion of soot:

$$\Delta n_{CO_2} = \Delta C_{CO_2} \cdot 10^{-6} \frac{V}{V_M} \tag{1}$$

where V_M is the molar volume of an ideal gas (24.5 L.mol^{-1} at 20°C and 1013 bar) and ΔC_{CO2} the CO_2 concentrations variation measured (in ppm) in the cell consecutively to sensor's regeneration.

During the oxidation of soot, 1 mole of carbon reacts with 1 mole of O_2 to give 1 mole of CO_2. Therefore, the mass of carbon "m_C" having served, after combustion, to vary the CO_2 concentration of a ΔC_{CO2} value in the sensor cell can be expressed as follows:

$$m_c = \Delta C_{CO_2} \cdot 10^{-6} \frac{V}{V_m} M_C \tag{2}$$

with M_C the molar mass of carbon equal to 12 g.mol^{-1}.

The variations in pressure and temperature being neglected, we can then connect linearly the mass of carbon m_C and the variation of CO_2 concentration in the cell ΔC_{CO_2} so that:

$$m_c = a \, \Delta C_{CO_2} \tag{3}$$

with factor "a" being defined by:

$$a = \frac{V}{V_m} 10^{-6} M_C = 0.196 \pm 0.004 \, \mu g. ppm^{-1} \tag{4}$$

The uncertainty on the mass determined can, then, be expressed by:

$$u(m_c) = \sqrt{\left(u_{\Delta C_{CO_2}}\right)^2 + (u_a)^2} \tag{5}$$

With $u_{\Delta C_{CO_2}}$ the uncertainty on ΔC_{CO_2} and u_a on the factor "a".

3 °) the last step of this protocol consists in weighing the resistive sensor after regeneration using the microbalance (Sartorius MC210P). Difference between sensor mass before and after regeneration could then be used to determine the mass of soot m_C oxidized during the regeneration step.

3. <u>RESULTS AND DISCUSSIONS</u>

3.1. Experimental data and analysis of the measurement of the CO_2 variation

In order to determine whether there is a bias in the concentration measured by the CO_2 sensor, regeneration of the soot-free sensor is carried out.

The protocol illustrated on figure 6 in the case of a soot-free sensor has been applied and will be used also for sensors loaded with soot (with t_0 considered as the time at the beginning of the CO_2 sensor's signal acquisition):

a) Continuous flow by purified and filtered dry compressed air, in the sensor cell at 1 L.min^{-1}, is injected in the measuring cell using critical orifices and a pump. The pump is triggered 120 s after the start of the acquisition (t_0). This sequence lasts long enough to renew the air in the cell. Taking into account the volume of the cell (0.4 L) and the flow rate, the renewal time is of the order of 40 s. Then, an air sweep time of the network of 240 s is considered sufficient to retrieve an air free of combustion gases. The signal from the humidity sensor integrated within the CO_2 sensor allows the renewal step to be checked since relative humidity is almost zero at the end of the air-sweeping phase of the dry network.

The pump is stopped at t_0 + 360 s and the system is isolated with the upstream and downstream 2-way valves, and the cell is then stabilized during 360 s.

b) Regeneration is triggered at t_0 + 720 s under static air conditions (no air flow).

c) Regeneration is stopped at t_0 + 860 s.

d) Data acquisition is stopped after 1800 s.

The analysis of these data makes it possible to estimate the difference in CO_2 concentration marked by two phases during measurement:

- ✓ The mean CO_2 concentration in the measuring cell is determined before the regeneration phase between 500 and 600 s (horizontal red arrow in figure 6),
- ✓ The mean CO_2 concentration in the measuring cell is determined after the regeneration phase, waiting for the signal stabilization (horizontal blue line in figure 7 and 8, around 1500-1600 s),
- ✓ The concentration difference (ΔC_{CO2}) from the averages obtained during these two phases as well as the uncertainty on this difference u (ΔC_{CO2}) expressed by:

$$u(\Delta C_{CO2}) = \sqrt{\left(u_{repetability}\right)^2 + \left(\left(\sqrt{2}\, u_{gain}\, \Delta C_{CO2}\right)\right)^2} \tag{6}$$

with $u_{repetability}$ the repeatability uncertainty = 10 ppm and u_{gain} the uncertainty of gain= 0.01.

The repeatability uncertainty (static error) corresponds to the noise amplitude of 10 ppm reported by the CO_2 sensor for a soot free resistive sensor after several measurements. The gain uncertainty was determined thanks to the CO_2 sensor calibration curve performed for CO_2 concentrations ranging from 0 to 1000 ppm at a relative humidity between 3% and 5% and at room temperature (24°C). It corresponds to 2 times the standard deviation of the calibration curve's slope. Both uncertainties are determined in a confidence level of 95%.

Figure 6 shows the signals provided by the CO_2 sensor during the regeneration of a soot-free sensor. At the end of regeneration, a rapid decrease followed by an abrupt increase in the CO_2 concentration could be noticed. Finally, the CO_2 signal regained its state before the regeneration.

In the absence of soot, we do not notice any significant difference between the CO_2 concentration signal before and after regeneration with a $\Delta C_{CO2} = 0$ ppm (horizontal red and blue lines at the same value of 1005 ppm taking into account the uncertainty of 10 ppm).
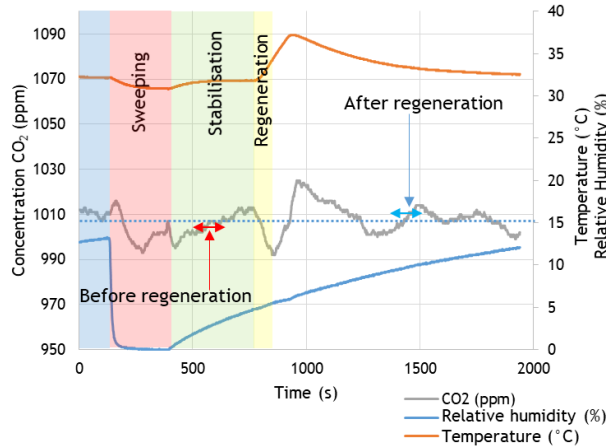

Figure 6: Response of the CO_2 sensor during regeneration of the soot-free resistive sensor

We represent in figure 7 the response of the CO_2 sensor for 48 µg of weighed mass (11.25 µg of calculated mass) and 120 µg of weighed mass (81.63 µg of calculated mass) of Mini-CAST soot deposited on the sensitive surface of the sensor and lost during the regeneration stage. For these two masses, the CO_2 concentration differences calculated before and after regeneration waiting for CO_2 concentration stabilization (red and blue lines) are respectively equal to 56 ± 10 ppm and 406 ± 11 ppm.
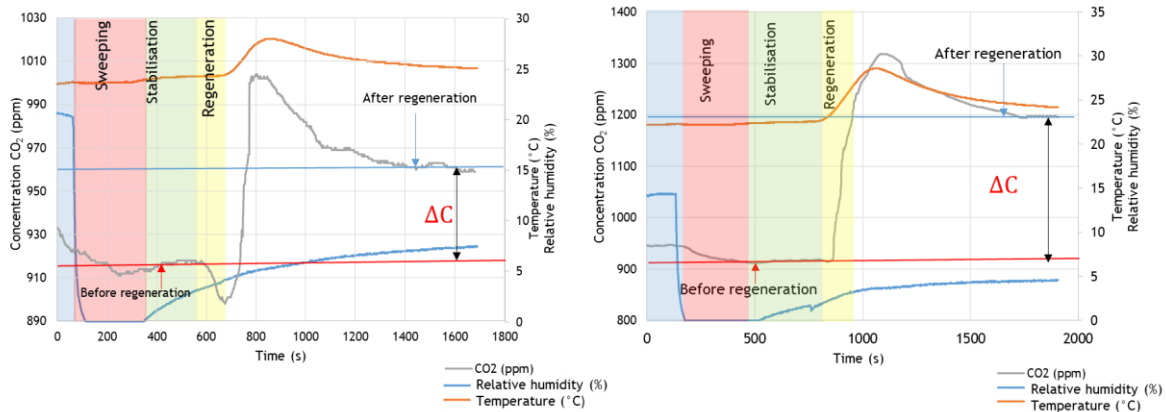
Figure 7: Response of the CO₂ sensor to the combustion of a) 48 µg of weighed mass (11.25 µg of calculated mass) and b) 120 µg of weighed mass (81.63 µg of calculated mass) of Mini-CAST soot during the regeneration of the contaminated sensor

The same protocol is used to study the response of the measuring cell during the regeneration of the soot sensor contaminated by TBP/HTP soot.

Figure 8.a shows the signal delivered by the CO_2 sensor for low quantities of soot produced by TBP/HTP, approximately 15 µg of weighed mass (3.74 µg of calculated mass), still deposited on the sensitive face of the resistive sensor before regeneration. We find the same form for the CO_2 concentration signal: a stable signal at first, followed by a decrease when regeneration begins and then an increase and finally stabilization of the concentration at the end of the regeneration. The difference in CO_2 concentrations (ΔC_{CO2}) is then estimated at 19 ± 10 ppm.

Figure 8.b shows the signal delivered by the CO_2 sensor for larger quantities of soot produced by the combustion of TBP/HTP. We notice similar evolution of the CO_2 concentration signal with stable steps before and after regeneration of the soot sensor corresponding to a concentration difference of 861 ± 21 ppm for a weighed mass of approximately 160 µg (169.58 µg of calculated mass), confirming the ability of this system to quantify soot deposit.
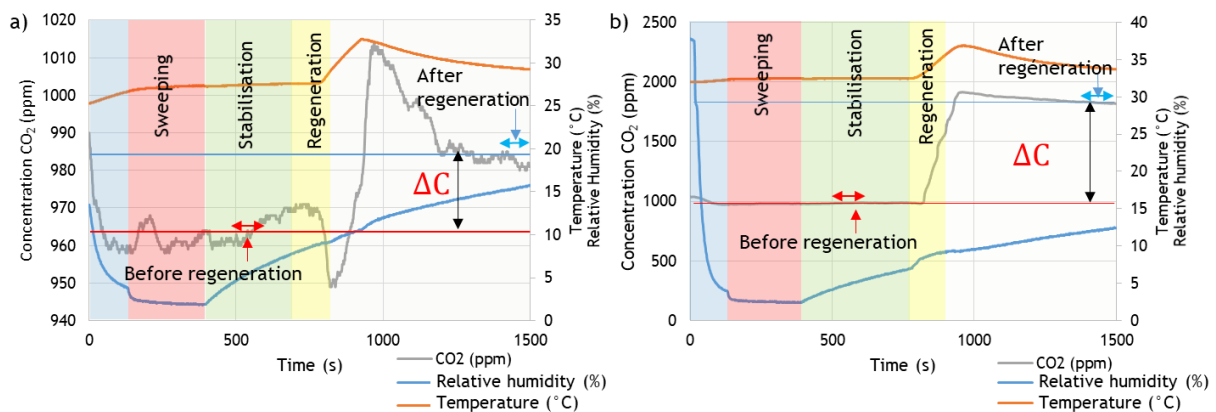

Figure 8: Response of the loaded CO₂ sensor to: a) 15 µg of weighed mass (3.74 µg of calculated mass) and b) 160 µg (169.58 µg of calculated mass) produced by combustion of TBP/HTP

3.2. Prediction curve: instrumental approach

Regenerations and CO_2 quantifications of sensors contaminated by several masses have been conducted and corresponding results are summarized in figure 9 for soot produced with Mini-CAST and from the combustion of TBP/HTP. Three tests were performed for each type of soot.

Figure 9 shows the evolution of the mass of carbon calculated from the difference of CO_2 concentrations (see equation 3) according to the weighed sensor mass variation before and after regeneration of sensor contaminated with these two types of soot.
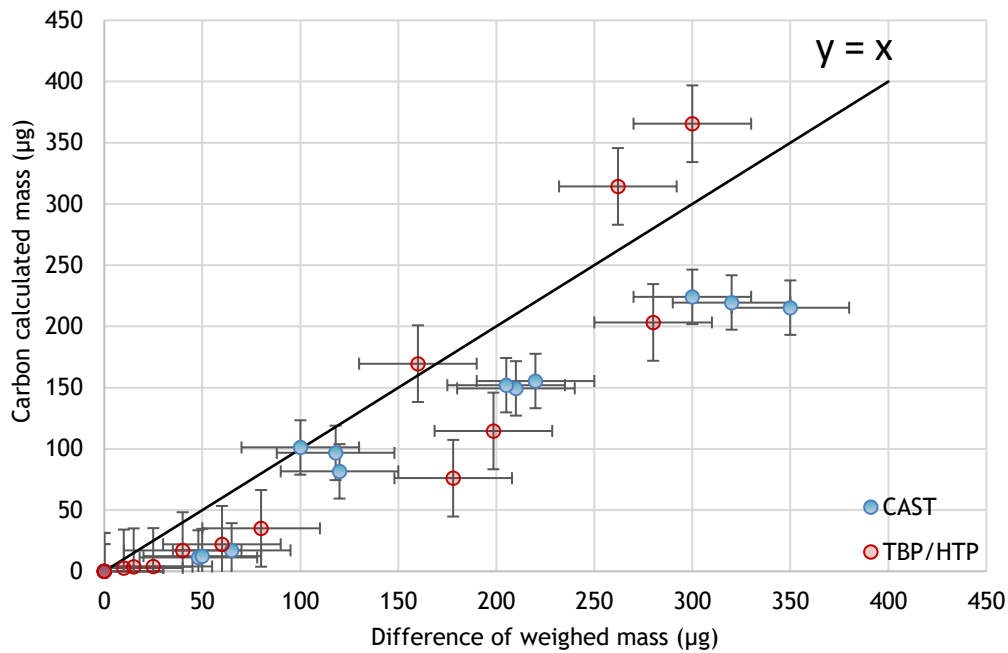
8

The carbon calculated mass is globally underestimated (in regard to linear proportional hypothesis), especially for Mini-CAST soot. The errors regarding the linear relationship vary between:

- 18 and 84 % for masses under 100 µg;
- 4 and 57 % for masses above 100 µg.

This underestimation can be explained by three assumptions:

• The first hypothesis is the presence of other species than CO_2. In fact, soot particles from Mini-CAST and TBP/HTP do not exclusively generate CO_2 during their oxidation. In fact, on the x-axis are represented differences in weighed soot while on the y-axis, we exclusively calculate the mass of carbon. Referring to the TGA curves (figure 3 and figure 4) and results obtained in figure 9, this assumption is not preponderant since the underestimation of carbon calculated mass should be more important in the case TBP/HTP (presence of other species more visible in TGA curves),

• the second hypothesis is an heterogeneous CO_2 concentration distribution over the cell, with either a potential accumulation of CO_2 in the dead zones or around the resistive sensor (CO_2 source) leading to an underestimation of the CO_2 sensor measurements.

• the third hypothesis is a loss of soot particles during the sensor mounting in the cell and during the sensor regeneration due to the pressure of formed CO_2 that induces expulsion of particles without overcoming combustion. It has been experimentally observed through the transparent glass cell when turning on the heater. Moreover, after the combustion of a low part of the deposited soot remains on the substrate. We believe, it is a reliable hypothesis to explain a big part of the observed uncertainty.

The soot produced by TBP/HTP present more dispersed results than those reported for Mini-CAST soot. This dispersion could be explained by a greater variability of the soot generation process in the test bench described by (Lintis et al., 2021). In addition, the TGA mass loss curves reported for TBP/HTP soot (figure 4) are more complex, in particular for the low temperatures which may explain the generation of different amounts of CO_2 during the regeneration process. Since the calculated masses of carbon are globally underestimated compared to the theoretical curve calibration (see figure 9), we propose in figure 10 a prediction curve for soot produced by the Mini-CAST and by the combustion of TBP/HTP. An empirical power-type correlation is thus introduced in order to predict the deposited masses as a function of the variations in CO_2 concentrations measured by the gas sensor. Within the dataset, and considering the dispersion for each type of soot, the proposed correlation seems to be relevant for both types of soot and we cannot discern the quantification results of Mini-CAST and TBP/HTP soot particles. Such agreement supports the TGA results and the fact that these two soot mainly produced CO_2 during

their oxidation, highlighting the relevance of this quantification method for particles mostly made of carbon, oxygen and hydrogen.
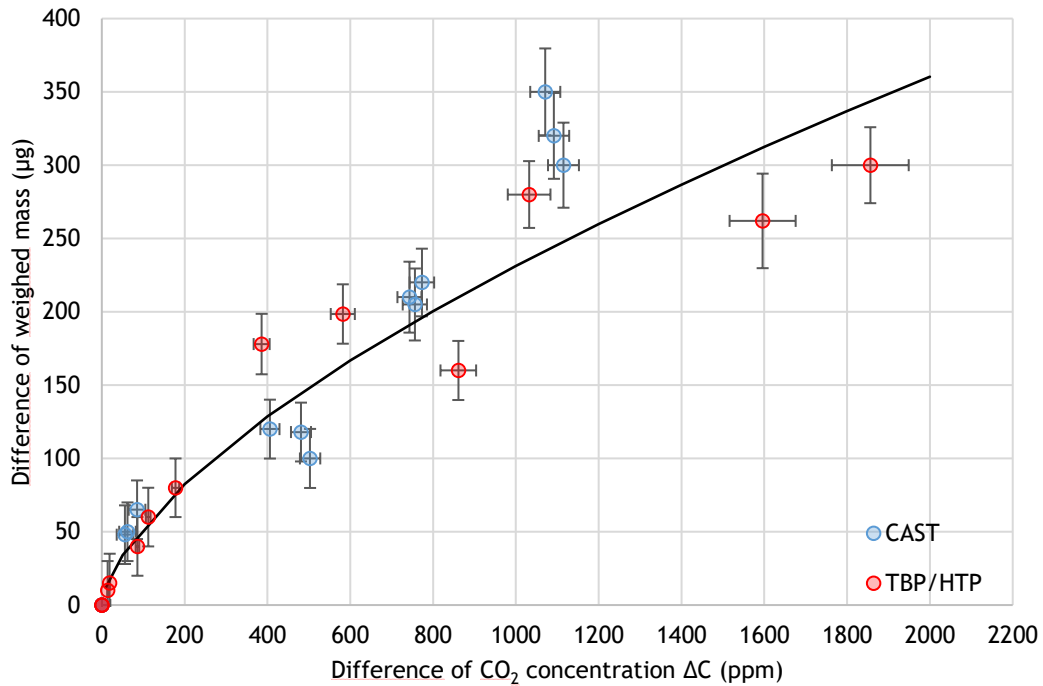
Figure 10 : Prediction curve for soot produced by the Mini-CAST and TBP/HTP combustion

The parameters of this curve were determined using a power function and applying a weighing uncertainty using OriginPRO 8.0.

$$m = cte \ \Delta C^b$$
(7)

with m the difference in the weighed masses of soot, cte = 2.78 ± 1.02 µg.ppm^{-b} and b = 0.64 ± 0.05.

The "CO_2 emission" method allows the quantification of high deposited masses up to 350 µg which could led to saturation of the electrical conductance of the resistive sensor as considered in our previous study (Kort et al., 2021).

3.3. Discussion

In our previous paper (Kort et al., 2021), we developed a sensing methodology based on "electrical conductance" measurement to characterize soot deposition dynamics on the wall of nuclear basic installation. The method gave good results for "low masses" between 2.8 µg and 19.6 µg corresponding to surface deposit of 230 – 1630 mg/m²) but sensor's asymptotic behavior was rapidly observed for TBP/HTP soot which is not compatible with the expected deposited mass during realistic nuclear fire. Therefore, the method presented in this paper, based on CO_2 emission measurement of oxidized deposited soot, allowed us to reach higher masses and can be complementary to the "electrical conductance" one. In this paper, the method was successfully calibrated for mass deposits from 15 µg to 350 µg corresponding to surface deposit of 1304 -28525 mg/m². The methods were both based on a calibration towards references of masses, OC-EC analyzer for the "electrical conductance" method developed in previous paper and microbalance for the present method. To make sure that they give results in accordance with each other, masses of both soot, compatibles with both methods (typically between 15 and 20 µg) were deposited on the sensor substrate.

For that purpose, the soot were not deposited manually and the resistive sensor was exposed for a period of one hour using the test bench previously used for the "Electrical Conductance" quantification method of Mini-CAST soot (Kort et al., 2021) (by applying a polarization voltage of 10 V). Final conductance was measured and the sensor was regenerated in the sensor cell for measuring CO_2 concentrations (before and after regeneration).

By applying the protocol explained previously, the difference in CO_2 concentration was calculated from the response of the CO_2 sensor for the Mini-CAST soot. For this configuration, we obtain a concentration difference

of 21 ± 10 ppm. Using the prediction curve for the mass deposited as a function of this difference in concentration (equation (2)), the mass deposited determined by the "CO_2 emission" method is then 19.8 ± 7.0 µg.

We applied the same protocol, using soot produced by the combustion of TBP/HTP for 1 hour. For this configuration, we obtain a CO_2 concentration difference of 17 ± 10 ppm. Using the prediction curve (equation 2), we find a mass deposited by the "CO_2 emission" method of 17.1 ± 6.1 µg.

Furthermore, the conductance obtained at the end of a one hour exposure were used to determine the deposited masses associated with the "electrical conductance" method. The masses quantified in the case of electrical conductance method were calculated from (Kort et al., 2021) by considering the conductance reached after one hour of exposure of 2440 ± 50 µS for soot from Mini-CAST soot and 870 ± 30 µS for TBP/HTP soot. Nevertheless, for the later soot, an underestimation of the deposited mass is expected since, contrary to sensors exposed to Mini-CAST soot and presented in our previous study (Kort et al., 2021), a saturation of the electrical conductance has been experimentally reported for the TBP/HTP case.

The masses quantified in the same experimental conditions by the two methods and for both types of soot are summarized in table 1. "Electrical conductance" and "CO_2 emission" methods gave coherent results in the case of Mini-CAST soot taking into account measurement uncertainties of both methods. In contrast, the values obtained for the TBP/HTP soot are not comparable and a factor of nearly 2.5 is noticed. This result is consistent with the saturation of the electrical conductance signal after exposure of the sensor to high masses of TBP/HTP soot, confirming the relevance of the CO_2 emission method for those samples.

Table 1: Mass deposited on the resistive sensor exposed for 1 hour to soot from Mini-CAST and TBP/HTP, quantified with the two measurement methods.

Quantified mass after a sensor exposition of 1 h at 10 V	Electrical conductance	CO_2 emission
Mini-CAST soot	14.4 ± 1.6 µg	19.8 ± 7.0 µg
TBP/HTP soot	6.7 ± 1.2 µg	17.1 ± 6.1 µg

As expected for CAST soot, the two measurement methods are complementary. Indeed, the first method of "electrical conductance" measurement can be used for masses up to 20 µg of deposited soot while the second method "CO_2 emission" can be used in the case of deposited masses greater than 16 µg (corresponding to differences in CO_2 concentration greater than the measurable limit of 15 ppm). In addition, this second method can be used both for Mini-CAST and TBP/HTP soot for deposited masses superior to 15 µg i.e. 1304 mg.m^{-2} on the sensitive surface of the resistive sensor.

Corresponding range of deposited mass of soot particles reported during real scale fires and measurement ability of both methods are compared in figure 11. Considering the mean deposited mass on the wall of a room exposed to fire in nuclear facility 1000-25 000 mg.m^{-2} estimated during real fire tests (Kort et al., 2019; Decoster, 2017; Mensch & Cleary, 2018; Riahi, 2012), we can thus conclude that for large-scale quantification, "CO_2 emission" method is rather to be privileged since maximum CO_2 concentration detectable by CO_2 sensor corresponds to a deposited mass of 28525 mg.m^{-2}.
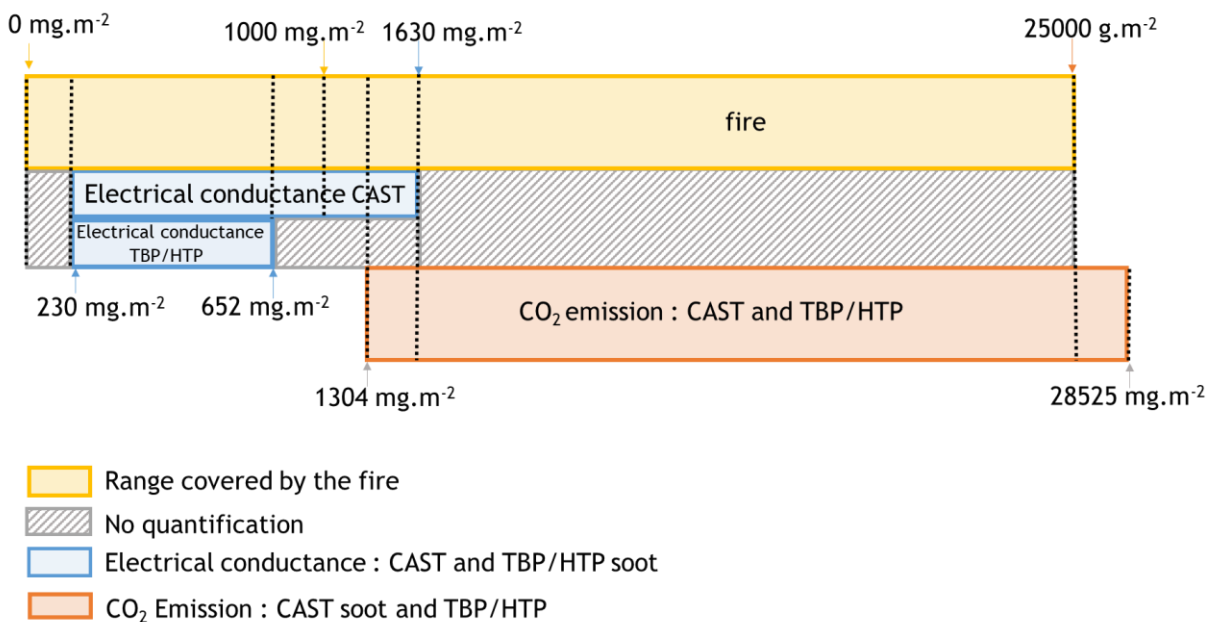

Figure 11 : Ranges of measurable masses for the different measurement methods

4. <u>CONCLUSION AND OUTLOOK</u>

The aim of this work was to present a soot quantification method that can be used for real scale fire.

This method is based on CO_2 emission measurement during the regeneration phase, using the heating element of a resistive sensor contaminated by soot particles. Thermogravimetric analyses coupled with the analysis of gases emitted by mass spectrometry, have revealed two main pieces of information. The combustion of Mini-CAST and TBP/HTP soot occurs at a temperature between 650 and 700 ° C and the main gas emitted during combustion is CO_2. Therefore, the use of a CO_2 sensor appeared a relevant solution for the measurement of gaseous species concentration emitted by the combustion of soot deposited on the sensitive face of the resistive sensor.

This method has a higher detection limit than the first quantification method proposed by (Kort et al., 2021) based on the measurement of the electrical conductance of the soot sensor, but it will be less effective at detecting low masses.

We have shown proof of feasibility of this second method "CO_2 emission" for two types of soot. Moreover, we have proposed a prediction curve for deposited masses which vary between 16 and 350 µg (1304 and 28525 mg.m^{-2}) depending on the measured CO_2 concentration. We discussed the applicability of this measurement method to realistic industrial fire situation and the mass range covered is wide and suitable for this application. It is possible to increase the inter-electrode space to reduce the sensitivity of the resistive sensor and thus quantify larger masses with the electrical conductance method. But, these changes lead to a recalibration of the resistive sensors for the electrical conductance method.

Calibration between the information delivered by the gas sensor (CO_2 concentration) and the mass deposited on the sensitive surface of the resistive sensor, considering representativeness of the mass deposited on an equivalent surface near the sensor, is then made possible. We demonstrated that deposited masses can be evaluated by a gas concentration measurement. A next step is to obtain deposited masses representative of the mass deposited on an equivalent surface near the sensor and to confirm the non-invasive behavior of such system regarding deposition mechanisms. Since thermophoresis (connected to the thermal conductivity of the sensor itself) is a major phenomenon of the deposition rate and that flow conditions are particularly complex in the boundary layer of walls of rooms experiencing fire conditions, this remains a challenge.

The objective of "quasi real-time" quantification can be achieved using this method as part of a multi-sensor approach, and several perspectives emerge regarding the "real-time" consideration. This regeneration-based method does not allow continuous monitoring of a deposit in a room on fire. Nevertheless, it allows to have, after calibration, a dynamic monitoring (quasi-real time, regarding the duration of regeneration/measurement cycle) of the deposited mass, usable for in situ measurements in representative fire conditions by using a suitable sampling system. A solution to have a real continuous monitoring would be to use two systems with time-shifted working mode: when one is under regeneration in gas sensor chamber, the second one is under fire conditions (soot exposure).

<u>REFERENCES</u>

Brugière, E., Gensdarmes, F., Ouf, F. X., Yon, J., & Coppalle, A. (2014). Increase in thermophoretic velocity of carbon aggregates as a function of particle size. *Journal of Aerosol Science*, *76*, 87–97. https://doi.org/10.1016/j.jaerosci.2014.06.007

Decoster, L. (2017). *Contribution à l'étude et à la modélisation du dépôt des suies lors d'un incendie*. Thèse de doctorat de l'Université d'Aix-Marseille.

Decoster, L., Coppalle, A., Ouf, F.-X., & Thiry, A. (2017). Measurements on Smoke Generated from an Office Fire: Soot Mass Concentration, Wall Deposition and Particle Characterization. *15th International Conference on Fire and Materials*.

Gelain, T., Porcheron, E. ., Chagnot, C., Doyen, I., Journeau, C., & Roulet, D. (2021). Development and validation of an agglomeration model for CFD simulations of aerosol dispersion in the frame of Fukushima fuel debris retrieval. *Journal of Nuclear Science and Technology*, 690–703. https://doi.org/10.1080/00223131.2020.1862717

Grondin, D., Breuil, P., Viricelle, J. P., & Vernoux, P. (2015). Development of a particulate matter sensor for diesel engine. *Procedia Engineering*. https://doi.org/10.1016/j.proeng.2015.08.838

Grondin, D., Geara, S., Breuil, P., Viricelle, J. P., & Vernoux, P. (2016). Influence of Electrodes Polarization on the Response of Resistive Soot Sensor. *Procedia Engineering*. https://doi.org/10.1016/j.proeng.2016.11.124

Kort, A., Ouf, F.-X., Gelain, T., Malet, J., Lakhmi, R., Breuil, P., & Viricelle, J.-P. (2019). Quantification spatiale du dépôt de suies dans un local lors d'un incendie. *Congrès Français sur les Aérosols*. https://doi.org/10.25576/ASFERA-CFA2019-16672

Kort, A., Ouf, F. X., Gelain, T., Malet, J., Lakhmi, R., Breuil, P., & Viricelle, J. P. (2021). Quantification of soot deposit on a resistive sensor: Proposal of an experimental calibration protocol. *Journal of Aerosol Science*, *156*(December 2020), 105783. https://doi.org/10.1016/j.jaerosci.2021.105783

Lintis, L., Ouf, F.-X., Parent, P., Ferry, D., Laffon, C., & Vallières, C. (2021). Quantification and prediction of water uptake by soot deposited on ventilation filters during fire events. *Journal of Hazardous Materials*, *403*, 123916. https://doi.org/https://doi.org/10.1016/j.jhazmat.2020.123916

Mensch, A., & Cleary, T. (2018). A Soot Deposition Gauge for Fire Measurements. *NIST Technical Note 1985*. https://doi.org/10.6028/NIST.TN.1985

Mensch, A., & Cleary, T. (2019). Measurements and predictions of thermophoretic soot deposition. *International Journal of Heat and Mass Transfer*, *143*.

Müller, J. O., Su, D. S., Jentoft, R. E., Kröhnert, J., Jentoft, F. C., & Schlögl, R. (2005). Morphology-controlled reactivity of carbonaceous materials towards oxidation. *Catalysis Today*, *102–103*, 259–265. https://doi.org/10.1016/j.cattod.2005.02.025

Ouf, F.-X., Mocho, V.-M., Pontreau, S., Wang, Z., Ferry, D., & Yon, J. (2015). Physicochemical properties of aerosol released in the case of a fire involving materials used in the nuclear industry. *Journal of Hazardous Materials*, *283*, 340–349. https://doi.org/10.1016/j.jhazmat.2014.09.043

Overholt, K. J., Floyd, J. E., & Ezekoye, O. A. (2016). Computational Modeling and Validation of Aerosol Deposition in Ventilation Ducts. *Fire Technology*, *52*(149–166). https://doi.org/10.1007/s10694-014-0414-5

Peacock, R. D., Cleary, T. G., Reneke, P. A., & Murphy, D. C. (2012). *A Literature Review of the Effects of Smoke from a Fire on Electrical Equipment*. http://www.nrc.gov/reading-rm.html.

Plagge, M., Krause, U., Da Riva, E., Schäfer, C., & Forkel-Wirth, D. (2017). An alternative method for thermal plume-induced aerosol release and deposition calculations in large geometries using fireFoam. *Nuclear Technology*, *198*(1), 43–52. https://doi.org/10.1080/00295450.2017.1291227

Riahi, S. (2012). *Development of Tools for Smoke Residue and Deposition Analysis*. the Faculty of The School of Engineering and Applied Science of The George Washington University in partial satisfaction of the requirements for the The George Washington University.

Zepper, E. T., Brown, A. L., Pierce, F., Voskuilen, T., & Louie, D. (2017). Contaminated Fuel Fires : Parametric Sensitivity of Resuspension and Boiling Particle Evolution. *Proceedings of the 2nd Thermal and Fluid Engineering Conference*, 1–15.